TITLE

TRPA1 channels are a source of calcium-driven cardiac mechano-arrhythmogenicity

AUTHORS

Breanne A Cameron[1]

Matthew R Stoyek[1]

Jessi J Bak[1]

T Alexander Quinn[1,2]

AFFILIATIONS

[1]Department of Physiology and Biophysics, Dalhousie University, Halifax, Canada

[2]School of Biomedical Engineering, Dalhousie University, Halifax, Canada

SUMMARY PARAGRAPH

Physiological systems require feedback to maintain normal function. In the heart, electrical excitation causes mechanical contraction[1], with feedback of mechanics to electrics occurring through 'mechano-electric coupling' processes[2]. In diseases that affect cardiac mechanics, this feedback can result in deadly mechanically-induced arrythmias ('mechano-arrhythmogenicity')[3]. However, the molecular identity of the specific factor(s) driving mechano-arrhythmogenicity are unknown[4]. Here we show that mechano-sensitive[5-10] transient receptor potential kinase ankyrin 1 (TRPA1) channels[11] are a source of cardiac mechano-arrhythmogenicity through a calcium (Ca^{2+})-driven mechanism. Using a cell-level approach involving stretch of single ventricular myocytes combined with simultaneous voltage-Ca^{2+} imaging, we found that activation of TRPA1 channels resulted in an increase in diastolic Ca^{2+} load and the appearance of stretch-induced arrhythmias, which were driven by trans-sarcolemmal fluxes and intracellular oscillations of Ca^{2+}, and prevented by pharmacological TRPA1 channel block or Ca^{2+} buffering. Our results demonstrate that TRPA1 channels act as a trigger for stretch-induced excitation (*via* Ca^{2+}-influx) and create a substrate for complex arrhythmic activity (*via* Ca^{2+}-overload), and thus may represent a novel anti-arrhythmic target in cardiac diseases in which TRPA1 channel expression and activity are augmented[12-16].

MAIN TEXT

Feedback is an essential element of biological function and is fundamental to its regulation and adaptation at all levels of physiological integration. The heart is an electro-mechanical pump in which electrical excitation of cardiac myocytes causes their contraction through a feedforward mechanism involving triggered release of calcium (Ca^{2+}) from intracellular stores, known as 'excitation contraction coupling'[1]. Feedback involves the impact of the mechanical state of cardiac myocytes on their electrical activity, by a process that has been termed 'mechano-electric coupling'[2]. In diseases involving changes in the mechanical state of the heart (such as an increase in hemodynamic load or altered cardiac mechanics), mechano-electric coupling may instead be a contributor to deadly disturbances of heart rhythm through mechanically-induced changes in cardiac electrophysiology[3], an effect we are calling 'mechano-arrhythmogenicity'. While the impacts of mechano-electric coupling on cardiac electrophysiology are well established[2], the molecular identity of the specific factor(s) involved, especially those driving mechano-arrhythmogenicity, have not been clearly defined[4].

Here we present a cell-level approach for investigating mechanisms of mechano-arrhythmogenicity, which allows us to overcome limitations of whole heart and tissue preparations by the precise control of single cell mechanical load with a carbon fibre-based system[17]. This is combined with simultaneous dual-parametric fluorescence imaging of transmembrane voltage and intracellular Ca^{2+} or video-based measurement of sarcomere dynamics, along with pharmacological interrogation of the suspected mechanisms driving arrhythmias that occur with cell stretch. Recent results from rabbit isolated heart studies in our lab suggest that ventricular mechano-arrhythmogenicity in acute regional ischemia (that occurs with blockage of a coronary artery) is caused by a mechano-sensitive Ca^{2+}-driven mechanism, facilitated by temporal

uncoupling of voltage-Ca^{2+} dynamics due to relative differences in action potential and Ca^{2+}-transient shortening by ATP-sensitive potassium (K_{ATP}) channel activation[18]. This creates a vulnerable period (VP) for Ca^{2+}-driven arrhythmias during late repolarisation, as Ca^{2+} remains high in repolarizing cells[19] (this has also been shown to occur during beta-adrenergic stimulation in failing human hearts[20]). In the present study, we utilised our single cell system to investigate the specific role of a K_{ATP}-induced VP in the susceptibility to stretch-induced arrhythmias, and to determine mechanisms underlying mechano-arrhythmogenicity.

K_{ATP} channels were activated by application of pinacidil (50 μM), an agonist of sulfonylurea receptor (SUR)2A/K_{ir}6.2 in cardiac and skeletal muscle[21]. To assess effects on the relative timing of recovery of voltage and Ca^{2+} and the size of the resulting VP, we simultaneously recorded action potentials and Ca^{2+} transients in electrically-paced (1 Hz), contracting, single rabbit ventricular myocytes under carbon fibre control using a single-excitation/dual-emission fluorescence imaging approach comprised of a single camera-optical splitter system[22] (Fig. 1a). With superfusion of a pinacidil-containing solution, there was a proportionally larger shortening of action potential duration (APD) than Ca^{2+} transient duration (CaTD; Fig. 1b), resulting in a significant increase in the VP (Fig. 1c) that was similar to that measured previously in the whole heart during acute ischemia[18,19]. These changes stabilised after 5 min, as no further change in APD, CaTD, or the VP were observed, nor was there a change under physiologic conditions over time (Fig. 1b, 1c).

Having increased the VP in our isolated cells by K_{ATP} channel activation with pinacidil, next we sought to determine whether this resulted in an increase in mechano-arrhythmogenicity with cell stretch during the VP. Rapid, transient stretch, mimicking systolic stretch of patho-physiologically non-contracting tissue in the heart, was applied to single cells by moving carbon fibres adhered to either end of the cell with piezo-electric translators (20, 30 or 40 μm applied and

removed at a rate of 0.7 μm/ms, for a total stretch time of 110-180 ms; resulting forces and stretched sarcomere lengths shown in Extended Data Fig. 1). Stretch was timed from the pacing stimulus to occur during the VP or during mid-diastole (Fig. 2a) in cells exposed to either physiologic or pinacidil-containing solution. Stretch resulted in a variety of arrhythmia types (revealed by tracking of sarcomere length), including premature ventricular contractions (PVCs, defined as 1 or 2 unstimulated contractions after stretch; Fig. 2b and Supplementary Video 1) and more complex arrhythmic behavior (*i.e.*, missed beats [Fig. 2c], asystole [2 or more missed beats; Fig. 2d, Supplementary Video 2], or sustained activity that either spontaneously resolved [Fig. 2e] or was terminated by an additional stretch [Fig. 2f, Supplementary Video 3]). The incidence of arrhythmic activity was much greater in pinacidil-treated cells than in control, but surprisingly was equally high for stretch applied during the VP or in diastole (Fig. 3a, b and Extended Data Fig. 2). As previous work in the whole heart has shown that the magnitude of tissue deformation is a key determinant of arrhythmia induction[23], we assessed the impact of stretch magnitude on the incidence of arrhythmias. Increasing the piezo translator displacement from 20 to 40 μm resulted in an increase in the applied force and resulting sarcomere length (Extended Data Fig. 1), but did not increase arrythmia incidence (in control cells there were few arrhythmias with stretch in both the VP and diastole for all piezo displacements [Extended Data Fig. 2a], while in cells exposed to pinacidil there was a non-significant trend toward increased mechano-arrhythmogenicity with larger stretches [Extended Data Fig. 2b]). To rule out the possibility that arrhythmias were the result of stretch-induced cell damage, contractile function was assessed before and after stretch at each magnitude. In both control and pinacidil-treated cells, there was no difference in the rate of sarcomere shortening or percentage sarcomere shortening during contraction before and after stretch (Extended Data Fig. 3a, b), nor were there differences before and after the occurrence of

complex arrhythmias (Extended Data Fig. 3c, d), suggesting that no cell damage had occurred in either case.

The finding that pinacidil enhanced mechano-arrhythmogenicity in both the VP and diastole was unexpected, as we had hypothesised that the incidence of stretch-induced arrhythmias would be increased only in the VP. We thus sought to determine the source of the overall increase in mechano-arrhythmogenicity with pinacidil. While pinacidil is thought to be a specific activator of K_{ATP} channels, it has also been shown to increase the activity of transient receptor potential kinase ankyrin 1 (TRPA1) channels in HEK293 cells[24]. TRPA1 channels are inherently mechano-sensitive[5] (contributing to mechanically-activated currents in neurons[6] and vertebrate hair cells[7]), have been shown to be highly expressed and functional in mouse ventricular myocytes[25] and to drive changes in rhythm in response to mechanical stimulation in the *Drosophila* heart[8], and are important in a range of cardiovascular functions and pathologies[12]. If TRPA1 channels are also present and functional in the rabbit heart and their activity is enhanced by pinacidil and stretch, they could account for the observed increase in mechano-arrhythmogenicity seen in our experiments. Using immunofluorescence, we found strong sarcolemmal expression of TRPA1 channels in our rabbit isolated ventricular myocytes (Extended Data Fig. 4). To determine if they play a role in mechano-arrhythmogenicity, we applied a non-specific blocker of mechano-sensitive channels (streptomycin[26]; 50 μM, 5 min of superfusion) and a specific antagonist for TRPA1 channels (HC-030031[27]; 10 μM, 30 min of incubation), which has been shown to block mechanically-induced excitation of sensory neurons[21]. In pinacidil-treated cells, both streptomycin and HC-030031 reduced the incidence of stretch-induced arrhythmias in both the VP and diastole (Fig. 3a; arrythmia incidence remained negligible control cells, Extended Data Fig. 5a). Importantly, streptomycin and HC-030031 appeared to have no other functional effects, as

contractile function was preserved with their application (Extended Data Fig. 5b). To confirm that TRPA1 channel activation may be a source of increased mechano-arrhythmogenicity, we specifically increased its activity by application of the TRPA1 channel-specific agonist allyl isothiocyanate (AITC; 10 μM, 5 min of superfusion)[28], which enhances its response to mechanical stimulation[9], and compared the incidence of arrhythmias with stretch in diastole to control and pinacidil-treated cells. In cells exposed to AITC, arrythmia incidence was greater than in control and pinacidil-treated cells, an effect that was eliminated by HC-030031 (Fig. 3b).

While the above results suggested that mechano-sensitive TRPA1 channels may act as a trigger for stretch-induced PVCs, the source of the complex arrhythmias seen with stretch remained unclear. TRPA1 channels preferentially pass Ca^{2+} into cells[29] and have been shown to cause an increase in diastolic Ca^{2+} concentration in ventricular myocytes[30], which can create an arrhythmogenic substrate[31] and further activate TRPA1 channels[32]. To investigate whether an increase in diastolic Ca^{2+} might be involved in the increase in mechano-arrhythmogenicity seen in our experiments, we measured intracellular Ca^{2+} concentration using a ratiometric fluorescence technique, which showed that both pinacidil and AITC increased Ca^{2+} in diastole (Fig. 3c). Interestingly, in AITC-treated cells this increase was eliminated by blocking TRPA1 channels with HC-030031 but in pinacidil-treated cells it was not (Fig. 3c), suggesting that the increase in diastolic Ca^{2+} with pinacidil occurs through a different mechanism. To assess whether intracellular calcium loading played a role in the observed arrhythmias, we buffered intracellular calcium with BAPTA (1 μM, 20 min of incubation), which reduced arrhythmias in both pinacidil- and AITC-treated cells (Fig. 3a, b). To further explore potential sources of the arrhythmogenic increase in cytosolic Ca^{2+} in pinacidil-treated cells, we stabilised ryanodine receptors in their closed state with dantrolene (1 μM, 5 min of superfusion) to reduce sarcoplasmic reticulum Ca^{2+} leak[33], however

this did not reduce arrythmia incidence. In control cells, the incidence of stretch-induced arrhythmias remained negligible with exposure to BAPTA or dantrolene and there was no effect on the rate of sarcomere shortening with contraction, however there was a slight decrease in the amount of sarcomere shortening, presumably due to an impact on sarcoplasmic reticulum calcium release (Extended Data Fig. 5). With an increase in intracellular Ca^{2+}, there is also the potential that diastolic stiffening of our isolated ventricular myocytes may have further contributed to the concomitant increase in mechano-arrhythmogenicity by either enhancing mechano-transduction or causing an increase in the force applied during stretch. However, there was no effect of pinacidil on stiffness or contractility (measured from the end-diastolic or end-systolic force length relationship in contracting cells; Extended Data Fig. 6a, b), nor was there a difference in the force applied during stretch between control and between pinacidil-treated cells (Extended Data Fig. 1a, b) or between cells in which stretch did or did not cause a complex arrythmia (Extended Data Fig. 6c), suggesting that changes in cell mechanics were not involved. Ultimately, the most explicit evidence for a direct role of Ca^{2+} in the observed arrhythmias came from dual voltage-Ca^{2+} fluorescence imaging, which revealed that during complex arrythmias, oscillations in intracellular Ca^{2+} precede changes in voltage (Fig. 4a, Supplementary Video 4).

Taken together, our results suggest that TRPA1 channels are a source of Ca^{2+}-driven cardiac mechano-arrhythmogenicity. Figure 4b summarises our working model of the role that TRPA1 channels play in triggering stretch-induced excitation and creating a substrate for more complex arrhythmic activity. As has been recently shown for transient receptor potential vanilloid-4 (TRPV4) channels in mouse hearts[34], TRPA1 channels are mechano-sensitive and allow Ca^{2+} to enter myocytes when stretched. The influx of Ca^{2+} will depolarise cell membrane potential, which if sufficiently large, will cause excitation and PVCs. At the same time, if constitutively active,

Ca^{2+} passing through TRPA1 channels will result in an increase in intracellular Ca^{2+} concentration, which may depolarise membrane potential *via* electrogenic forward-mode sodium-Ca^{2+} exchanger current, bringing the cell closer to the threshold for excitation, while also creating an arrhythmia sustaining substrate[31]. Further, TRPA1 channel activity itself is directly modulated by intracellular Ca^{2+} levels, in a bimodal fashion, such that an increase in Ca^{2+} will potentiate inward Ca^{2+} current, thus increasing the contribution of TRPA1 to mechano-arrhythmogenicity, but at certain levels will inactivate channels, thus limiting the degree of Ca^{2+} overload and preventing cell damage[35]. In our experimental model, exposure to pinacidil either directly activated TRPA1 channels or did so indirectly *via* an increase in intracellular Ca^{2+}, while AITC caused direct activation. In both cases this would lead to an enhanced depolarising current during stretch (acting as a trigger for PVCs) and would increase intracellular Ca^{2+} concentration (acting as a substrate for mor complex arrhythmias). In this way, TRPA1 channels act as the central player in a feed-forward loop that increases Ca^{2+}-dependent mechano-arrhythmogenicity. The role of TRPA1 in the stretch-induced arrhythmias observed in our model is further supported by the reduction in their incidence with specific block of TRPA1 channels by HC-030031 or non-specific block of mechano-sensitive channels by streptomycin. Further, the contribution of Ca^{2+} influx as an arrhythmic trigger, and overload as a sustaining substrate, is supported by the reduction in stretch-induced arrhythmias with buffering of Ca^{2+} by BAPTA and block of TRPA1 channels by HC-030031.

These findings have potentially important implications for anti-arrhythmic treatments of cardiac diseases in which TRPA1 channel expression and activity are augmented[12]. This is especially true for diseases in which additional factors that activate TRPA1 channels are present (*e.g.*, oxidative stress[36]), as the response of TRPA1 channels to mechanical stimulation is enhanced by an increase in its baseline activity[9]. For instance, acute myocardial ischemia resulting from blockage of a

coronary artery is associated with TRPA1-mediated myocardial damage[13] and lethal ventricular arrhythmias that are thought to involve contributions of altered tissue mechanics, intracellular Ca^{2+} handling, and oxidative stress[37], so targeting TRPA1 channels in that setting could help prevent multiple detrimental outcomes (and perhaps even promote post-ischemic myocardial repair[14]). This may be also be true in chronic pathologies associated with changes in cardiac mechanics, intracellular Ca^{2+}, oxidative stress, and other TRPA1 modulating factors[11] in which lethal arrhythmias occur, such as ventricular pressure overload (TRPA1 inhibition has been shown to reduce hypertrophy and fibrosis in that setting[15]), making TRPA1 channels a novel anti-arrhythmic target with exciting therapeutic potential[16].

MAIN REFERENCES

1. Bers, D. M. Cardiac excitation-contraction coupling. *Nature*. **415**, 198-205 (2002).
2. Quinn, T. A. & Kohl, P. Cardiac mechano-electric coupling: acute effects of mechanical stimulation on heart rate and rhythm. *Physiol. Rev.* In Press (2021).
3. Quinn, T. A. The importance of non-uniformities in mechano-electric coupling for ventricular arrhythmias. *J. Interv. Card. Electrophysiol.* **39**, 25-35 (2014).
4. Peyronnet, R., Nerbonne, J. M. & Kohl, P. Cardiac mechano-gated ion channels and arrhythmias. *Circ. Res*. **118**, 311-29 (2016).
5. Moparthi, L. & Zygmunt P. M. Human TRPA1 is an inherently mechanosensitive bilayer-gated ion channel. *Cell Calcium* **91**, 102255 (2020).
6. Vilceanu, D. & Stukcy, C. L. TRPA1 mediates mechanical currents in the plasma membrane of mouse sensory neurons. *PLoS One* **5**, e12177 (2010).
7. Corey, D. P., *et al*. TRPA1 is a candidate for the mechanosensitive transduction channel of vertebrate hair cells. *Nature* **432**, 723-30 (2004).
8. Sénatore S., Reddy, V. R., Séméria, M., Perrin, L. & Lalevée, N. Response to mechanical stress is mediated by the TRPA channel painless in the *Drosophila* heart. *PLoS Genet.* **6**, e1001088 (2010).
9. Brierly S. M., *et al*. TRPA1 contributes to specific mechanically activated currents and sensory neuron mechanical hypersensitivity. *J. Physiol*. **589**, 3575-93 (2011).
10. Kerstein, P.C., del Camino, D., Moran, M. M., Stucky, C. L. Pharmacological blockade of TRPA1 inhibits mechanical firing in nociceptors. *Mol. Pain* **5**, 19 (2009).
11. Meents, J. E., Ciotu, C. I. & Fischer, M. J. M. TRPA1: a molecular view. *J. Neurophysiol.* **121**, 427-443 (2019).

12. Wang, Z. *et al*. The TRPA1 channel in the cardiovascular system: promising features and challenges. *Front. Pharmacol.* **10**, 1253 (2019).

13. Conklin, D. J., *et al*. TRPA1 channel contributes to myocardial ischemia-reperfusion injury. *Am. J. Physiol. Heart. Circ. Physiol.* **316**, H889-99 (2019).

14. Li, R., Liu, R., Yan, F., Zhuang, X., Shi, H. & Gao, X. Inhibition of TRPA1 promotes cardiac repair in mice after myocardial infarction. *J. Cardiovasc. Pharmacol.* **75**, 240-9 (2020).

15. Wang, Z. *et al*. TRPA1 inhibition ameliorates pressure overload-induced cardiac hypertrophy and fibrosis in mice. *E. Bio. Medicine* **36**, 54-62 (2018).

16. Moran, M. M. TRP channels as potential drug targets. *Annu. Rev. Pharmacol. Toxicol.***58**,309-30 (2018).

17. Iribe, G., Helmes, M. & Kohl, P. Force-length relations in isolated intact cardiomyocytes subjected to dynamic changes in mechanical load. *Am. J. Physiol. Circ. Physiol.* **292**, H1487-97 (2007).

18. Baumeister, P., *et al.* Mechanically-induced ventricular arrhythmias during acute regional ischemia. *J. Mol. Cell. Cardiol*. **124,** 87-8 (2018).

19. Tang, L., Joung, B., Ogawa, M., Chen, P. S. & Lin S. F. Intracellular calcium dynamics, shortened action potential duration, and late-phase 3 early afterdepolarization in Langendorff-perfused rabbit ventricles. *J. Cardiovasc. Electrophysiol.* **12**, 1364-71 (2012).

20. Lang, D., *et al*. Arrhythmogenic remodeling of β_2 versus β_1 adrenergic signaling in the human failing heart. *Circ. Arrhythm. Electrophysiol.* **8**, 409-19 (2015).

21. Fujita, A. & Kurachi, Y. Molecular aspects of ATP-sensitive K^+ channels in the cardiovascular system and K^+ channel openers. *Pharmacol. Ther.* **85**, 39-53 (2000).

22. Quinn, T. A., *et al*. Electrotonic coupling of excitable and nonexcitable cells in the heart revealed by optogenetics. *Proc. Natl. Acad. Sci. U S A.* **113**:14852-7 (2016).

23. Quinn, T. A., Jin, H., Lee, P. & Kohl, P. Mechanically induced ectopy via stretch-activated cation-nonselective channels Is caused by local tissue deformation and results in ventricular fibrillation if triggered on the repolarization wave edge (Commotio Cordis). *Circ. Arrhythm. Electrophysiol*. **10**, e004777 (2017).

24. Ma, L. H., *et al*. Pinacidil, a K_{ATP} channel opener, identified as a novel agonist for TRPA1. *Chinese Sci. Bull.* **57**, 1810-7 (2012).

25. Andrei, S. R., Sinharoy, P., Bratz, I. N. & Damron, D. S. TRPA1 is functionally co-expressed with TRPV1 in cardiac muscle: Co-localization at z-discs, costameres and intercalated discs. *Channels* **10**, 395-409 (2016).

26. White, E. Mechanosensitive channels: therapeutic targets in the myocardium? *Curr Pharm Des*. **12**, 3645-63 (2006).

27. McNamara, C. R. *et al*. TRPA1 mediates formalin-induced pain. *Proc. Natl. Acad. Sci. U S A.* **104**,13525-30 (2007).

28. Jordt, S-E., *et al*. Mustard oils and cannabinoids excite sensory nerve fibres through the TRP channel ANKTM1. *Nature*. **427**, 260-5 (2004).

29. Bobkov, Y. V., Corey, E. A, & Ache, B. W. The pore properties of human nociceptor channel TRPA1 evaluated in single channel recordings. *Biochem. Biophys. Acta.* **1808**, 1120-8 (2012).

30. Andrei, S. R. *et al*. TRPA1 ion channel stimulation enhances cardiomyocyte contractile function via a CaMKII-dependent pathway. *Channels* **11**, 587-603 (2017).

31. Landstrom, A. P., Dobrev D. & Wehrens, X. H. T. Calcium signaling and cardiac arrhythmias. *Circ. Res.* **120**, 1969-93 (2017).

32. Zurborg, S., Yurgionas, B., Jira, J. A., Caspani, O. & Heppenstall P.A**.** Direct activation of the ion channel TRPA1 by Ca2+. *Nat. Neurosci.* **10**, 277-9 (2007).

33. Hartmann, N., *et al*. Antiarrhythmic effects of dantrolene in human diseased cardiomyocytes. *Heart Rhythm* **14**, 412-9 (2017).

34. Veteto, A. B., Peana, D., Lambert, M. D., McDonald, K. S. & Domeier, T. L. Transient receptor potential vanilloid-4 contributes to stretch-induced hypercontractility and time-dependent dysfunction in the aged heart. *Cardiovasc. Res.* **116**, 1887-96 (2020).

35. Wang, Y. Y., Chang R. B., Waters, H. N., McKemy, D. D. & Liman, E. R. The nociceptor ion channel TRPA1 is potentiated and inactivated by permeating calcium ions. *J. Biol. Chem.* **21**, 32691-32703 (2008).

36. Andersson, D. A., Gentry, C., Moss, S. & Bevan, S. Transient receptor potential A1 is a sensory receptor for multiple products of oxidative stress. *J. Neurosci.* **28**, 2485-94 (2008).

37. Carmeliet, E. Cardiac ionic currents and acute ischemia: from channels to arrhythmias. *Physiol. Rev.* **79**, 917-87 (1999).

FIGURES

Figure 1 | Temporal uncoupling of voltage-calcium dynamics in isolated ventricular myocytes by activation of ATP-sensitive potassium channels with pinacidil. a, Representative trace of an action potential (AP, blue) and calcium transient (CaT, red) simultaneously recorded by fluorescence imaging in a rabbit isolated ventricular myocyte before (left) and after (right) 5 min of pinacidil exposure and the associated vulnerable period (VP, green). APD_{50}, action potential duration at 50% repolarisation; $CaTD_{80}$, calcium transient duration at 80% recovery; ECC, excitation-contraction coupling time. **b,** Average APD_{50} (blue) and $CaTD_{80}$ (red) over 10 min of normal Tyrode (NT, solid) or pinacidil (PIN, dashed) superfusion. **c,** Average VP over 10 min of NT or PIN superfusion. Differences assessed by one-way ANOVA, with Tukey *post-hoc* tests. $^{*}p<0.05$ for the change over time; $^{\#}p<0.05$ for the change over time compared to CaTD. Error bars represent standard error of the mean.

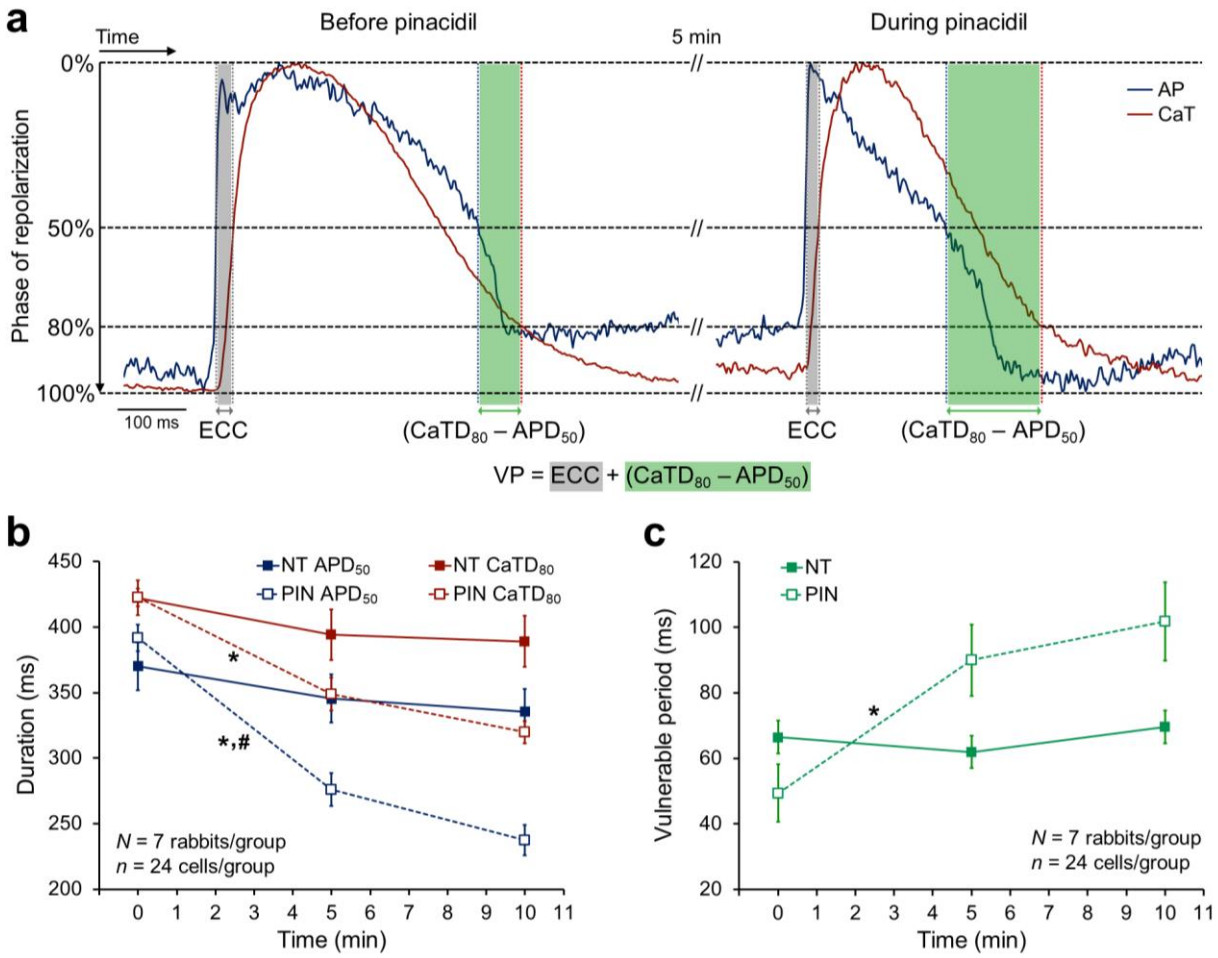

Figure 2 | Arrhythmias elicited by rapid, transient stretch of single ventricular myocytes. a, Representative measurement of sarcomere length in a rabbit isolated ventricular myocyte exposed to pinacidil during 1 Hz pacing (orange dots) and stretch in diastole and the VP (green segments of trace) that did not result in an arrhythmic event. **b,** Stretch-induced premature ventricular contraction (PVC, blue segment). **c,** Stretch-induced missed beat (red segment). **d,** Stretch-induced asystole. **e,** Stretch-induced sustained arrhythmic activity that spontaneously resolved. **f,** Stretch-induced sustained arrhythmic activity that was terminated by an additional stretch.

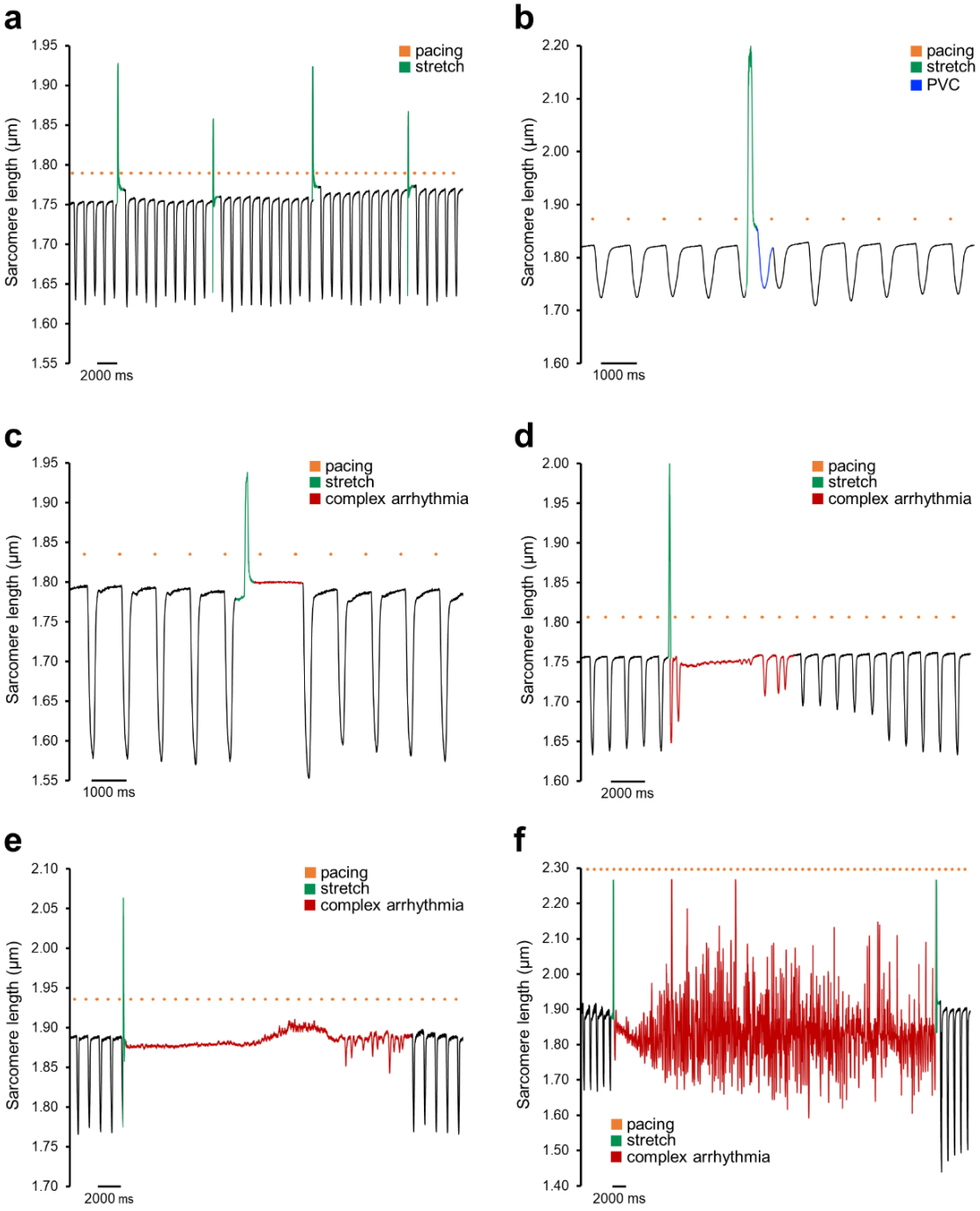

Figure 3 | Effects of pharmacological interventions on mechano-arrhythmogenicity. a, Incidence of premature ventricular contractions (PVC, blue) and complex arrhythmias (red) with rapid, transient stretch of rabbit isolated ventricular myocytes during diastole or the vulnerable period (VP) in cells exposed to: normal Tyrode (NT); pinacidil (PIN); PIN+BAPTA; PIN+dantrolene (DNT); PIN+streptomycin (STP); or PIN+HC-030031. Ca^{2+}, calcium; SAC, stretch-activated channels. **b,** Incidence of arrhythmias with stretch during diastole in cells exposed to: NT; PIN; allyl isothiocyanate (AITC); AITC+HC-030031; or AITC+BAPTA. Differences assessed using chi-square contingency tables and Fisher's exact test. *p<0.05 between groups. **c,** Average percent change in diastolic Ca^{2+} concentration compared to control in rabbit isolated ventricular myocytes exposed to: PIN; AITC; PIN+HC-030031; or AITC+HC-030031. Differences assessed using unpaired Student's t-test. *p<0.05 compared to control; $^{\#}p$<0.05 between groups. Error bars represent standard error of the mean.

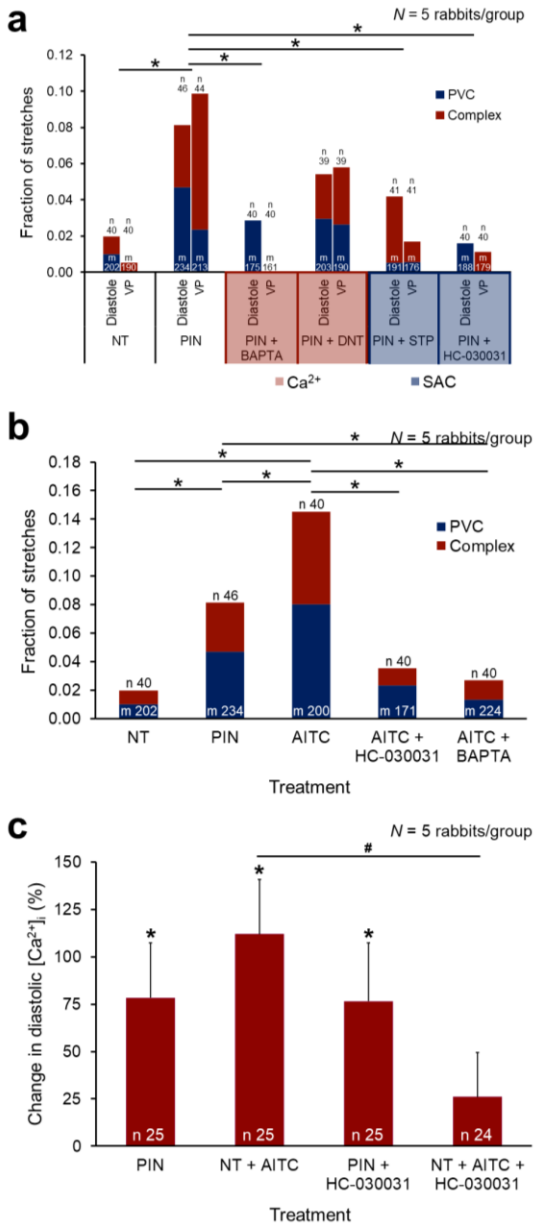

Figure 4 | Role of intracellular calcium (Ca^{2+}) and transient receptor potential kinase ankyrin 1 (TRPA1) channels in mechano-arrhythmogenicity. a, Representative trace of voltage (blue) and intracellular Ca^{2+} (red) simultaneously recorded by fluorescence imaging in a rabbit isolated ventricular myocyte exposed to pinacidil (PIN) before and after a rapid, transient stretch (green) that resulted in sustained arrhythmic activity. Inset shows intracellular Ca^{2+} oscillations preceding changes in voltage. **b,** Schematic representation of the mechanisms underlying Ca^{2+}-mediated mechano-arrhythmogenicity involving TRPA1 channels. AITC, Allyl isothiocyanate; PIN, pinacidil; PVC, premature ventricular contractions; STP, streptomycin.

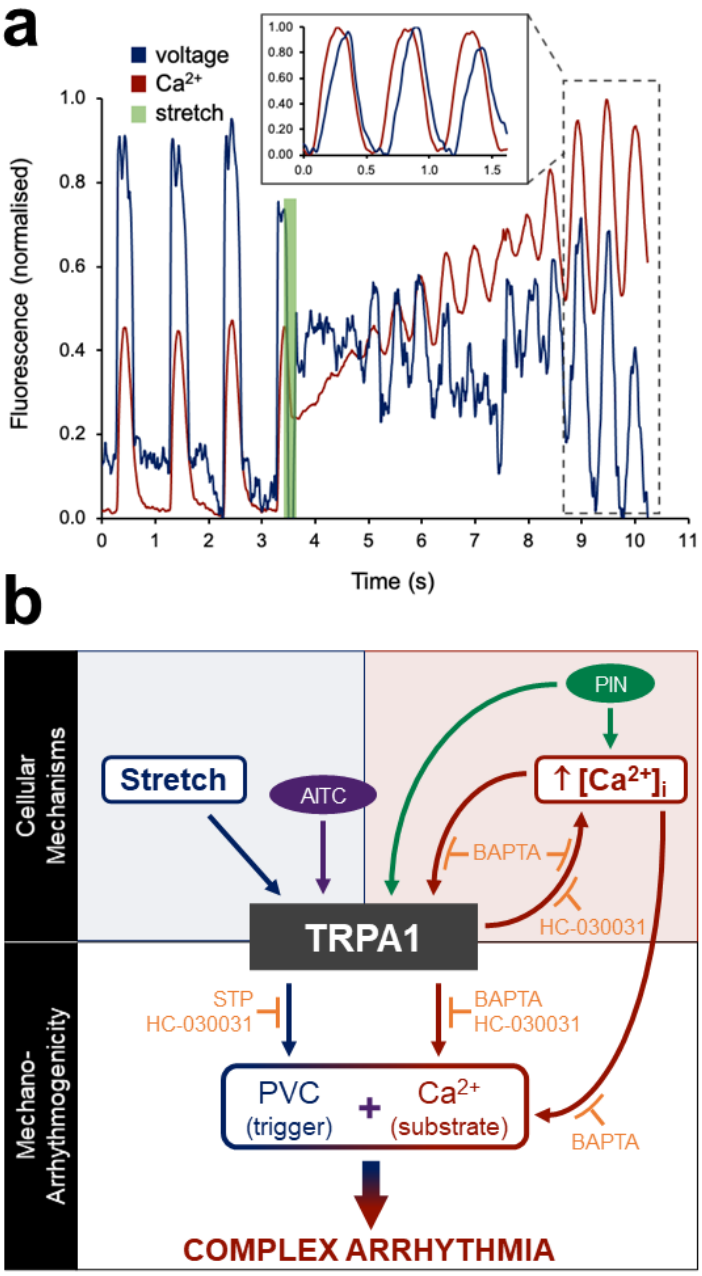

METHODS

Animal model. Experiments involved the use of female New Zealand White rabbits (2.1 ± 0.2 kg, Charles River) and were conducted in accordance with the ethical guidelines of the Canadian Council on Animal Care, with protocols approved by the Dalhousie University Committee for Laboratory Animals. Details have been reported following the Minimum Information about a Cardiac Electrophysiology Experiment (MICEE) reporting standard[38].

Cell isolation. Animals were euthanised by ear vein injection of pentobarbital (140 mg/kg) and heparin (1,500 units/kg, Sigma-Aldrich), followed by rapid excision of the heart, aortic cannulation, and Langendorff perfusion (20 mL/min) with 37°C normal Tyrode (NT) solution (containing, in mM: 120 NaCl, 4.7 KCl, 1.0 $MgCl_2$, 1.8 $CaCl_2$, 10 glucose, 10 HEPES [Sigma-Aldrich], with pH adjusted to 7.40 ± 0.05 with NaOH and an osmolality of 300 ± 5 mOsm) bubbled with 100% oxygen. After a rest period of 15 min, the perfusate was switched to calcium (Ca^{2+})-free solution (containing, in mM: 117 NaCl, 10 KCl, 1 $MgCl_2$, 10 creatine, 20 taurine, 5 adenosine, 2 L-carnitine, 10 glucose, 10 HEPES [Sigma-Aldrich], with pH adjusted to 7.40 ± 0.05 with NaOH and an osmolality of 300 ± 5 mOsm) with the addition of 0.018 mM EGTA (Sigma-Aldrich) for 5 min. The perfusate was then switched to digestion solution, comprised of Ca^{2+}-free solution with the addition of 200 U/mL Collagenase II (Worthington Biochemical Corporation), 0.06 mg/ml Protease XIV (from *Streptomyces griseus*, Sigma Aldrich), and 100 μM $CaCl_2$ for 5 min, at which point the perfusion rate was reduced to 15 mL/min until the heart became flaccid and jelly-like (~10-12 min). The left ventricular free wall was removed and placed into 50 mL of stop solution comprised of Ca^{2+}-free solution with the addition of 0.5 % BSA (Sigma Aldrich) and 100 μM $CaCl_2$. The tissue was agitated, the solution filtered through a 300 μm nylon mesh, the tissue

returned to fresh stop solution and re-agitated, and the solution filtered. The cell-containing filtered solution was divided into 2 mL microcentrifuge tubes (VWR) and maintained at room temperature.

Carbon fibre method. Cells were stretched by the carbon fibre (CF) method, adapted from previous work[5]. Briefly, a pair of CFs (12-14 μm in diameter, gift of Prof. Peter Kohl, Institute for Experimental Cardiovascular Medicine, University Heart Centre Freiburg / Bad Krozingen) were mounted with cyanoacrylate adhesive in borosilicate glass capillaries pulled from glass tubes (1.12 mm inner / 2 mm outer diameter, World Precision Instruments) and bent at 30° 1.2 mm from the end to allow near-parallel alignment of the CFs with the bottom of the experimental chamber. The left and right carbon fiber were trimmed to 1.2 mm and 0.6 mm in length from the end of the glass capillary, respectively, so that one CF was more compliant and the other more stiff. Each CF was mounted in a microelectrode holder (MEH820, World Precision Instruments) coupled to a three-axis water hydraulic micromanipulator (MHW-103, Narishige) and mounted on a linear piezo-electric translator (PZT, P-621.1CD, Physik Instrumente). The CF position was controlled by a piezo amplifier / servo controller (E-665.CR, Physik Instrumente) driven by a voltage signal generated from a DAQ device (USB-6361; National Instruments) dictated by custom-written routines in LabVIEW (National Instruments). Stiffness of the CFs was calculated by pressing a CF against a force transducer system (406A, Aurora Scientific), measuring the force for given displacements of the PZT, and fitting the data by linear regression to the formula: stiffness = force / PZT displacement. This allowed measurement of force applied during cell stretch by measuring CF bending through monitoring PZT and CF tip positions (described below) and applying the formula: force = stiffness × (change in distance between CF tips - change in distance between PZTs).

Single cell stretch. The cell-containing solution in a microcentrifuge tube was gently agitated with a transfer pipette and a small drop of solution was added to an imaging chamber (RC-27NE2, Warner Instruments) containing 1 mL of NT maintained at 35°C by a temperature controller (TC-344C, Warner Instruments) and mounted on an inverted fluorescence microscope (IX-73, Olympus) with a 40× objective (UPLFLN40X, Olympus). The surface of the coverslip on the bottom of the chamber was coated with poly-2-hydroxyethyl methacrylate (poly-HEMA, Sigma-Aldrich) to prevent cell adhesion. Once the cells had settled, 1 Hz bipolar electrical field stimulation (SIU-102, Warner Instruments) was commenced and normally contracting rod-shaped myocytes with clear striations and well-delineated membranes with no signs of blebbing were randomly selected. Electrical stimulation was stopped, and the CFs were positioned at either end of the long-axis of a cell and gently lowered onto the cell surface using the hydraulic micromanipulators. Adhesion of the cell to the CFs was confirmed by raising it off of the coverslip. Once cell attachment was established, electrical stimulation was recommenced, and cells were allowed to contract against the CFs for ~1-2 min to improve electrostatic interactions responsible for adhesion. Cells were then superfused at 2.1 mL/min through an inline heater (SF-28, Warner Instruments) with either NT or pinacidil containing solution (to activate ATP-sensitive potassium, K_{ATP}, channels) for 5 min. Transient stretch (~100 ms duration, 20 μm PZT displacement) was then applied during mid-diastole (600 ms delay after an electrical stimulus, as determined by simultaneous voltage-calcium imaging, described below), followed by a 10 s wait, stretch during the vulnerable period (VP, 150 ms delay), and after another 10 s wait, was repeated (see Fig. 2a for an example). This protocol was duplicated at increasing magnitudes of PZT displacement (30 and 40 μm), with 30 s between repetition, for a total of 12 stretches.

Assessment of stretch effects. Throughout the protocol, sarcomere length and PZT and CF tip positions were monitored and recorded at 240 Hz (Myocyte Contractility Recording System, IonOptix). From this, cell contractile function (rate and percentage of sarcomere shortening) and characteristics of cell stretch (applied force and change of sarcomere length) were measured. Arrhythmic activity was assessed from sarcomere length measurements, which revealed stretch-induced premature ventricular contractions (PVC, defined as 1 or 2 unstimulated contractions after stretch) or more complex arrhythmias (including missed beats, asystole [2 or more missed beats], and sustained arrhythmic activity that either spontaneously resolved or was terminated by an additional stretch (see Fig. 2 for examples of each). When a sustained arrhythmia occurred, the next stretch was delayed by the appropriate amount after it resolved (either 10 or 30 s). Any stretch that resulted in slippage of the CF, or a sustained arrhythmia occurred that did not spontaneously resolve or could not be terminated by a maximum of 2 stretches was excluded (< 1% of all cells), as cell damage may have occurred.

Pharmacological interventions. Pharmacologic agents dissolved in distilled water, dimethyl sulfoxide (DMSO), or ethanol as appropriate, were added to the perfusate and continuously perfused for 5 min before cell stretch. Agents included: BAPTA-AM (1 μM, to buffer intracellular Ca^{2+}, Abcam), dantrolene (1 μM, to stabilize ryanodine receptors, Abcam), streptomycin (50 μM, to non-specifically block stretch-activated channels, Sigma-Aldrich), HC-030031 (10 μM, to block transient receptor potential ankyrin 1, TRPA1, channels, Abcam), and allyl isothiocyanate (AITC, 10 μM, to activate TRPA1 channels, Sigma-Aldrich). For BAPTA-AM and HC-030031, cells were incubated for 20 or 30 min, respectively, prior to superfusion.

Dual parametric voltage-Ca^{2+} fluorescence imaging. For loading of cells with fluorescent dyes, 1 mL of the supernatant was removed from a microcentrifuge tube containing cells in stop solution

and replaced with 1 mL of NT. The Ca^{2+}-sensitive dye Fluo5-F, AM (5μM, ThermoFisher Scientific) and Pluronic F-127 (0.02 %, Biotium) dissolved in DMSO were added to the tube and the cells incubated in the dark for 20 min. The supernatant was then replaced with fresh NT, the voltage-sensitive dye di-4-ANBDQPQ (20 μm, University of Connecticut Health Centre) dissolved in ethanol was added to the tube and the cells were incubated in the dark for 14 min. The supernatant was again replaced with fresh NT, probenecid (1 mM, Sigma-Aldrich) was added to the tube, and the cells were maintained in the dark at room temperature. When ready for imaging, the solution containing dye-loaded cells was gently agitated with a transfer pipette and a small drop of solution was added to 1 mL of NT in the imaging chamber and the CFs adhered to a cell as described above (CFs reduced motion artefact associated with cell movement in the vertical plane during contraction, allowing measurements to be made without an excitation-contraction uncoupler). Fluorescence was excited by a mercury lamp (U-HGLGPS, Olympus) passed through a 466/40 nm bandpass filter (FF01-466/40, Semrock) and reflected onto the sample by a 495 nm dichroic mirror (FF495-Di03, Semrock). For simultaneous measurement of transmembrane voltage and intracellular Ca^{2+}, each fluorescent signal was projected onto one-half of a 128 × 128-pixel, 16-bit electron-multiplying charge-coupled device (EMCCD) camera sensor (iXon3, Andor Technology) using an emission image splitter (Optosplit II; Cairn Research) and recorded at 500 frames per second with 2 ms exposure time and maximum electron-multiplying gain. The two signals were split with a 685 nm dichroic mirror (FF685-Di02, Semrock) and Flou-5F emission was collected with a 525/50 nm bandpass filter (FF03-525/50, Semrock) and di-4-ANBDQPQ emission with a 700 nm long-pass filter (HQ700lp; Chroma Technology).

Analysis of voltage-Ca^{2+} signals was performed using custom routines in Matlab (R2018a, MathWorks). Fluorescence for each signal was averaged over the entire cell, a temporal filter (50

Hz low-pass Butterworth) was applied, and bleaching was eliminated by fitting the resulting signal with a second-order polynomial and subtracting the result. From the corrected signals, time to 50% or 80% recovery of the action potential (action potential duration, APD_{50} or APD_{80}) or the Ca^{2+} transient (Ca^{2+} transient duration, $CaTD_{50}$ or $CaTD_{80}$) were averaged over 3 consecutive cardiac cycles. The vulnerable period (VP) was calculated as the difference between $CaTD_{80}$ and APD_{50}, plus the difference between the timing of the action potential and Ca^{2+} transient upstrokes (excitation-contraction coupling time, ECC, see Fig. 1): $VP = ECC + (CaTD_{80} - APD_{50})$.

Ratiometric intracellular Ca^{2+} fluorescence imaging. Imaging of intracellular Ca^{2+} levels was performed using the ratiometric Ca^{2+}-sensitive dye Fura Red, AM (AAT Bioquest). Cells were loaded with the dye by incubating in the dark for 20 min with 5 μM of the dye, 0.02 % Pluronic F-127, and 1 mM probenecid dissolved in DMSO. Fluorescence was excited by alternating light pulses from two white light-emitting diodes (CFT-90-W; Luminus Devices), one with a 420/10 nm bandpass filter (FF01-420/10, Semrock) and the other with a 531/22 nm bandpass filter (FF02-531/22, Semrock), which were combined into the microscope excitation light path with a 455 nm dichroic mirror (AT455dc, Chroma Technology) and reflected onto the sample by a 562 nm dichroic mirror (T562lpxr, Chroma Technology). Fluorescence was measured through a 632/60 nm bandpass filter (AT635/60m, Chroma Technology) with the EMCCD camera at 500 frames per second with 2 ms exposure time and maximum electron-multiplying gain. Light pulses and camera frame acquisition were synchronised with a custom control box (provided by Dr. Ilija Uzelac, Georgia Institute of Technology) so that alternating frames corresponded to the signal generated by each of the two excitation wavelenghts[34]

Analysis of intracellular Ca^{2+} was performed using custom routines in Matlab. Fluorescence was averaged over the entire cell and a temporal filter (50 Hz low-pass Butterworth) was applied.

The two Ca^{2+} signals were separated and the ratio of the signals was calculated. Any remaining bleaching was eliminated by fitting the resulting signal with a second-order polynomial and subtracting the result. From the corrected signals, the minimum value for each cardiac cycle (representing diastolic Ca^{2+} concentration) was measured and averaged over 3 consecutive cardiac cycles.

Immunohistochemistry. Coverslips (22 mm round; VWR) were coated with laminin (100 µg/mL, diluted in PBS) and stored in a 12-well plate (VWR). Isolated myocytes (1 mL) in Ca^{2+}-free stop solution were added to each well and allowed to settle for 10 min. The supernatant was replaced with NT in two increments (50%, 100% of solution), with 10 min rest between each change. Myocytes were then maintained at room temperature to seed (3 hours).

Once fixed, plates were bathed in blocking solution (5% BSA [Sigma-Aldrich] in PBS with 0.1% Triton X-100 [Tx; Sigma-Aldrich]) at room temperature. After 1 hour, plates were transferred to 100 µL of a primary antibody storage solution (5%BSA/0.01%Tx in PBS) in a custom-built humidity chamber (glass petri dish lined with a PBS-soaked Kimwipe and sealed with Parafilm [VWR]). Diluted (1:200) primary antibody (mouse anti-rabbit TRPA1 Clone 6G8, Sigma-Aldrich) was placed on the parafilm (100uL) and the coverslip was mounted cell-side down and incubated at $4^{o}C$ for 1 hour. Coverslips were subsequently washed in quadruplicate (5 min each) with PBS (0.01%), and diluted (1:200) secondary antibody (goat anti-mouse IgG AlexaFluor 555 conjugate, Invitrogen) staining was performed as before with the addition of an actin marker (AlexaFluor 488 conjugated phalloidin, Abcam) diluted to 1:500. Following secondary antibody staining, coverslips were bathed in a 9:1 solution of glycerol:Tris buffer (pH 8.1) containing 2% n-propyl gallate (Sigma-Aldrich) with DAPI nuclear stain (0.5 µg/mL; Sigma-Aldrich).

Confocal Microscopy. Confocal imaging was performed using an LSM 710 confocal microscope (Zeiss Canada) with a 40x, 0.90 NA objective (LCI Plan-Neofluar, Carl Zeiss AG). Preparations were epi-illuminated with a mercury lamp (X-Cite 120Q; Lumen Dynamics) or with argon (405/488 nm) and helium-neon (543 nm) lasers. Prisms were set to collect emitted fluorescence in the 405-430, 480-520, and 530-585 nm bandpass ranges. Single optical plane images were processed using Zeiss Zen2009 software (1.5 digital zoom; 488 nm range: 55% power, 500 master gain, 1.0 digital gain, 0.0 digital offset, 1.0 AU pinhole; 555 nm range: 35% power, 650 master gain, 1.0 digital gain, 0.0 digital offset, 1.0 AU pinhole). Images were processed with Photoshop CS6 (Adobe Systems Inc).

Statistics. Statistics were performed using GraphPad Prism 8. Differences in arrhythmia incidence were assessed using chi-square contingency tables and Fisher's exact test. Differences between group means were assessed by two-tailed, paired or unpaired Student's t-test, one-way ANOVA with Tukey *post-hoc* tests (for normally distributed data), Kruskal-Wallis with Dunn's multiple comparisons test (for data that is not normally distributed), or Wilcoxon matched-pairs test, where appropriate. A p-value of < 0.05 was considered significant. Figures indicate the number of replicates used in each experiment (N = rabbits, n = cells, m = stretches).

Code availability. All custom computer source code used in this study is available from the corresponding author upon reasonable request.

Data availability. The datasets generated during and/or analysed during the current study are available from the corresponding author upon reasonable request.

METHODS REFERENCES

38. Quinn, T. A. *et al*. Minimum Information about a Cardiac Electrophysiology Experiment (MICEE): standardised reporting for model reproducibility, interoperability, and data sharing. *Prog. Biophys. Mol. Bio.* **107**,4-10 (2011).

STATEMENTS

Acknowledgements. We thank P. Kohl for specialty carbon fibres, G. Iribe and K. Kaihara for technical assistance with cell stretch, and I. Uzelac for technical assistance with electronic LED control. This work was supported by the Canadian Institutes of Health Research (MOP 342562 to T.A.Q.); by the Natural Sciences and Engineering Research Council of Canada (RGPIN-2016-04879 to T.A.Q.); by the Dalhousie Medical Research Foundation (T.A.Q.); by the Canadian Foundation for Innovation (32962 to T. A. Q.); and by the Heart and Stroke Foundation of Canada through a National New Investigator award (T.A.Q.).

Author contributions. B.A.C. and T.A.Q. designed the study, interpreted the data, and wrote the manuscript; B.A.C. performed the cell stretch and fluorescence imaging experiments and analysed the data; M.R.S. contributed to experimental design and setup and assisted with the immunohistochemical analysis; J.J.B. performed the immunohistochemical experiments and analysed the data. All authors read and approved the manuscript.

Author information. The authors declare no competing interests. Correspondence and request for materials should be addressed to T.A.Q. (alex.quinn@dal.ca).

EXTENDED DATA

Extended Data Figure 1 | Mechanical characteristics of cell stretch. a, Average applied force during rapid, transient stretch of rabbit isolated ventricular myocytes exposed to normal Tyrode (NT, black) or pinacidil (PIN, white) with increasing levels of piezo-translator movement (20, 30, and 40 μm). **b,** Average sarcomere length during stretch. Differences assessed by one-way ANOVA, with Tukey *post-hoc* tests. *$p < 0.05$ between groups. Error bars represent standard error of the mean.

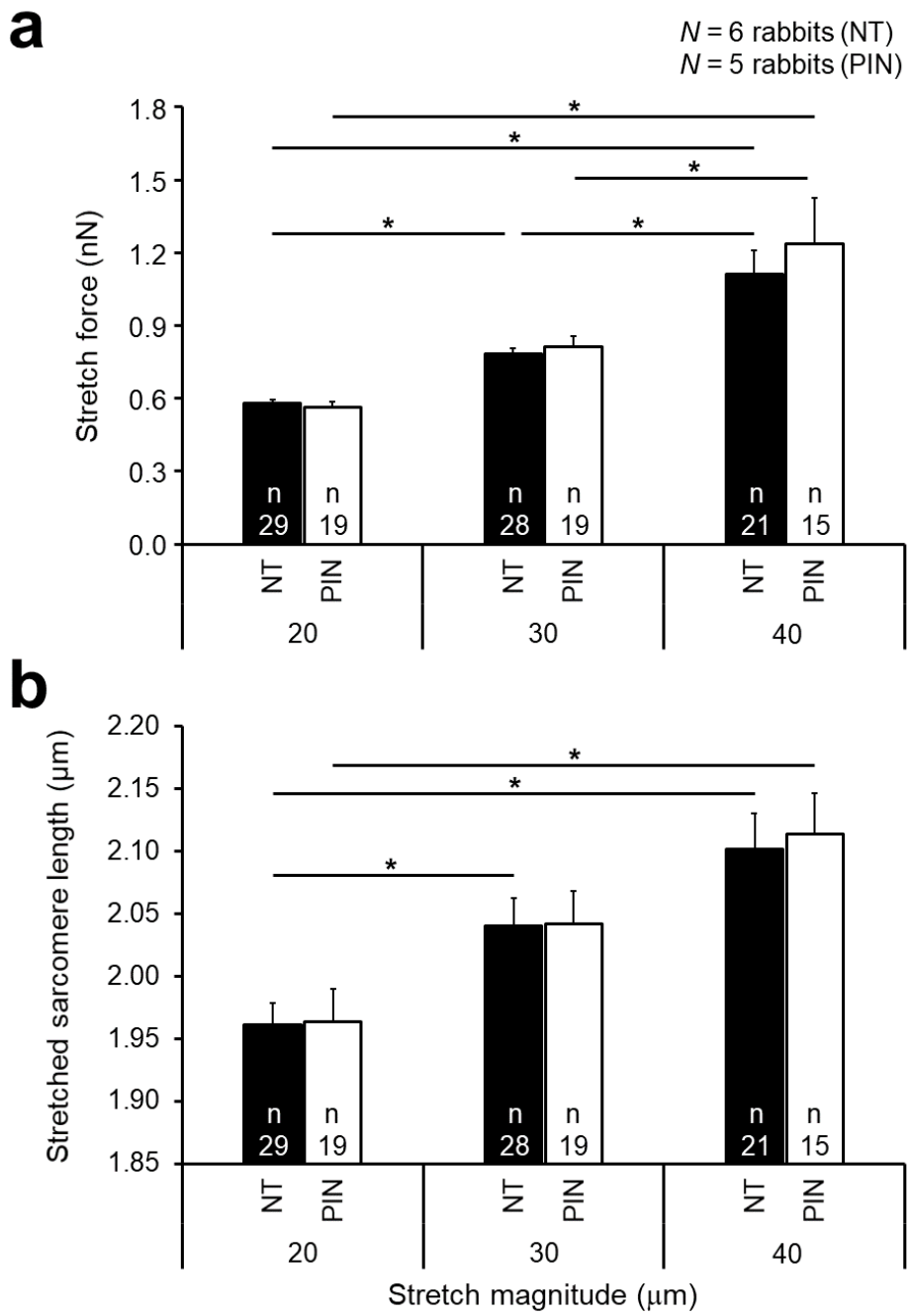

Extended Data Figure 2 | Effect of stretch magnitude on the incidence of mechano-arrhythmogenicity. a, Incidence of premature ventricular contractions (PVC, blue) and complex arrhythmias (red) with rapid, transient stretch during diastole (left) and the vulnerable period (VP, right) with increasing levels of piezo-translator movement (20, 30, and 40 μm) in rabbit isolated ventricular myocytes exposed to normal Tyrode (NT). **b,** Incidence of arrhythmias in cells exposed to pinacidil (PIN). Differences assessed using chi-square contingency tables and Fisher's exact test. *p< 0.05.

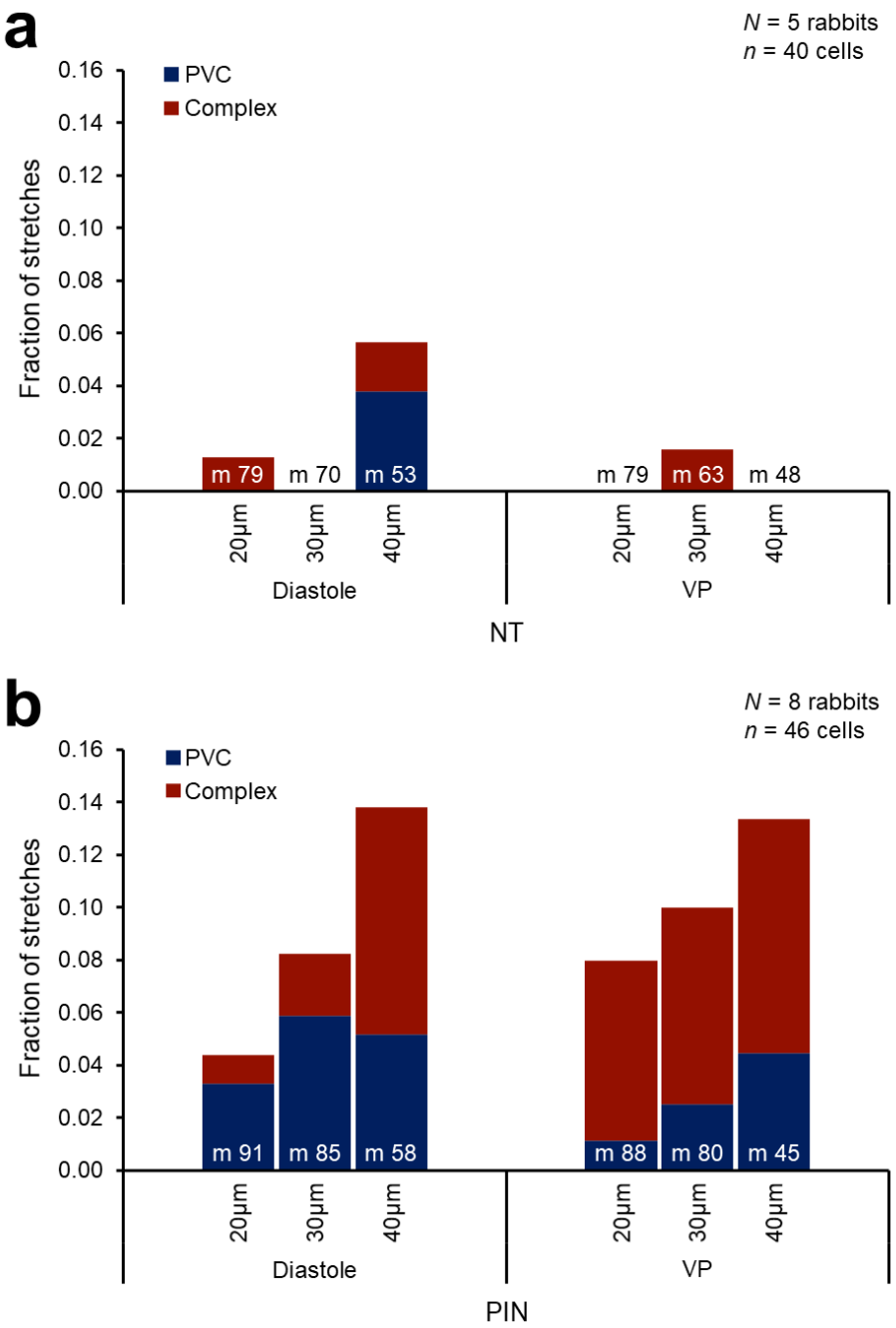

Extended Data Figure 3 | Effect of stretch magnitude and complex arrhythmias on contractile function. a, Average rate of sarcomere shortening during contraction of rabbit isolated ventricular myocytes exposed to normal Tyrode (NT, black) or pinacidil (PIN, white) before (baseline) and after rapid, transient stretch of increasing levels of piezo-element movement (20, 30, and 40 μm). **b,** Average percent sarcomere shortening. Differences assessed by one-way ANOVA, with Tukey *post-hoc* tests. **c,** Average rate of sarcomere shortening in cells exposed to pinacidil prior to a complex arrhythmia (green) and after its termination (red). **d,** Average percent sarcomere shortening. Differences assessed using two-tailed, paired Student's t-test. Error bars represent standard error of the mean.

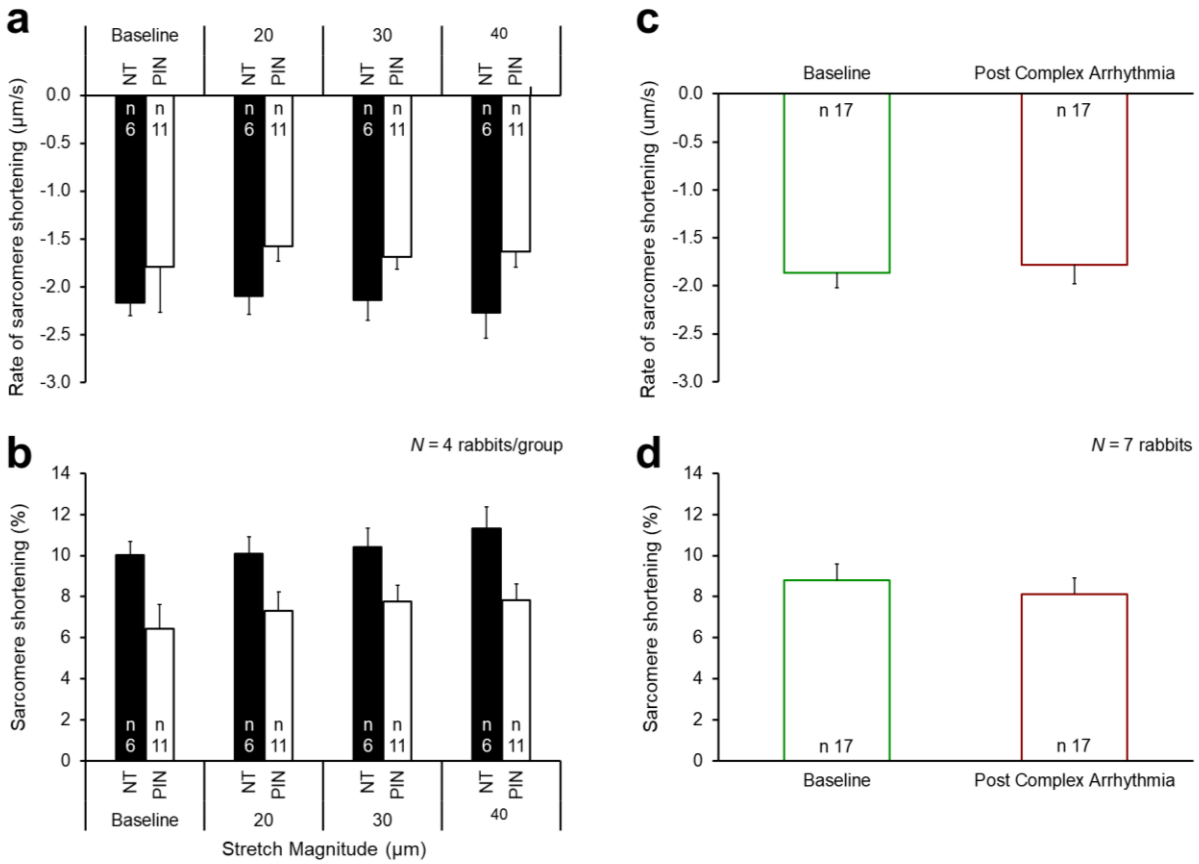

Extended Data Figure 4 | Expression of TRPA1 channels in rabbit isolated ventricular myocytes. Two-dimensional confocal image (40×) of an immuno-stained rabbit isolated ventricular myocyte showing TRPA1 (purple) and α-Actinin (green) expression. Yellow arrows indicate surface sarcolemmal expression and white arrows indicate t-tubular expression. DAPI was used for nuclear labelling (blue).

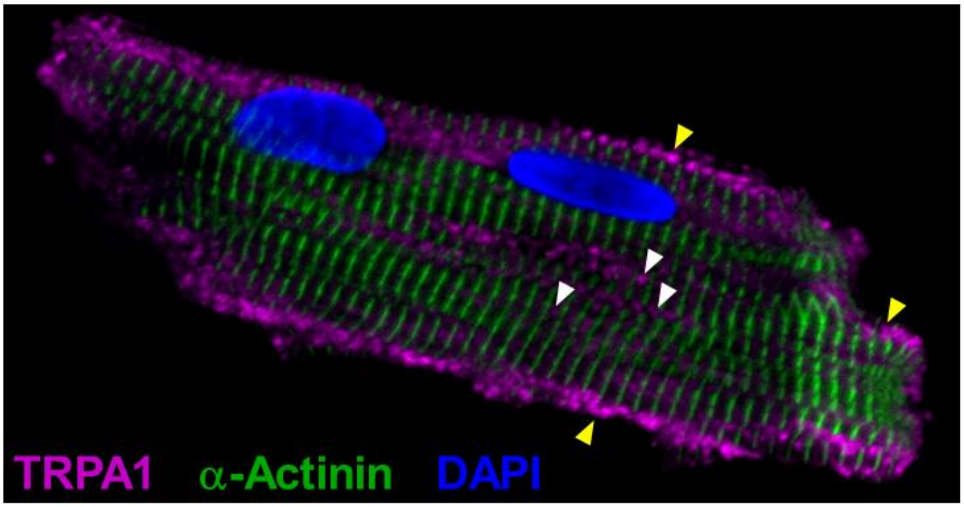

Extended Data Figure 5 | Effect of pharmacological interventions on mechano-arrhythmogenicity and contractile function in control conditions. a, Incidence of premature ventricular contractions (PVC, blue) and complex arrhythmias (red) with rapid, transient stretch during diastole or the vulnerable period (VP) in rabbit isolated ventricular myocytes exposed to: normal Tyrode (NT); NT+BAPTA; NT+dantrolene (DNT); NT+streptomycin (STP); or NT+HC-030031. Ca^{2+}, calcium; SAC, stretch-activated channels. Differences assessed using chi-square contingency tables and Fisher's exact test. **b,** Average rate of sarcomere shortening during contraction of rabbit isolated ventricular myocytes exposed to normal Tyrode (NT); NT+BAPTA; NT+dantrolene (DNT); NT+streptomycin (STP); or NT+HC-030031. Differences assessed by Kruskal-Wallis test. **c,** Average percent sarcomere shortening. Differences assessed by one-way ANOVA, with Tukey *post-hoc* tests. *p< 0.05. Error bars represent standard error of the mean.

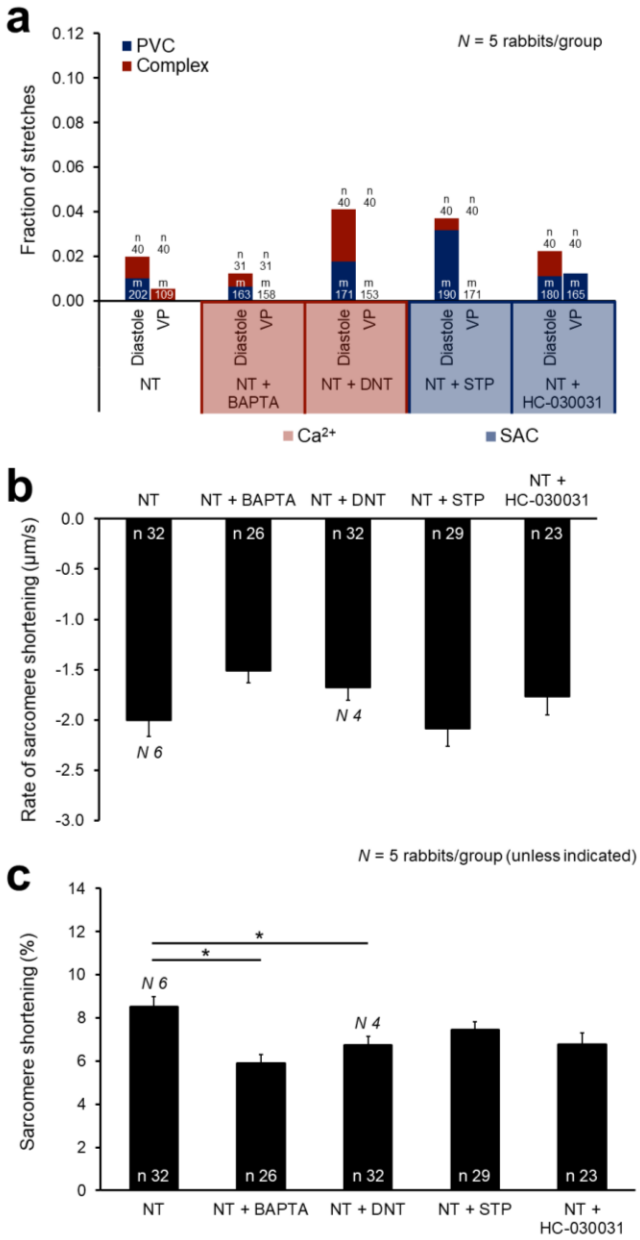

Extended Data Figure 6 | Effect of pinacidil on cell mechanics. a, Average stiffness of rabbit isolated ventricular myocytes exposed to normal Tyrode (NT, black) or pinacidil (PIN, white), measured from the slope of the end-diastolic force length relationship (EDFLR). **b,** Average elastance measured from the slope of the end-systolic force length relationship (ESFLR). Differences assessed using two-tailed, unpaired Student's t-test. **c,** Average applied force during rapid, transient stretch in diastole (left) or the VP (right) for stretches that did not affect rhythm (NSR, green) or resulted in a complex arrhythmia (ARR, red) within the same pinacidil-treated cells. Differences assessed using the Wilcoxon matched-pairs test. Error bars represent standard error of the mean.

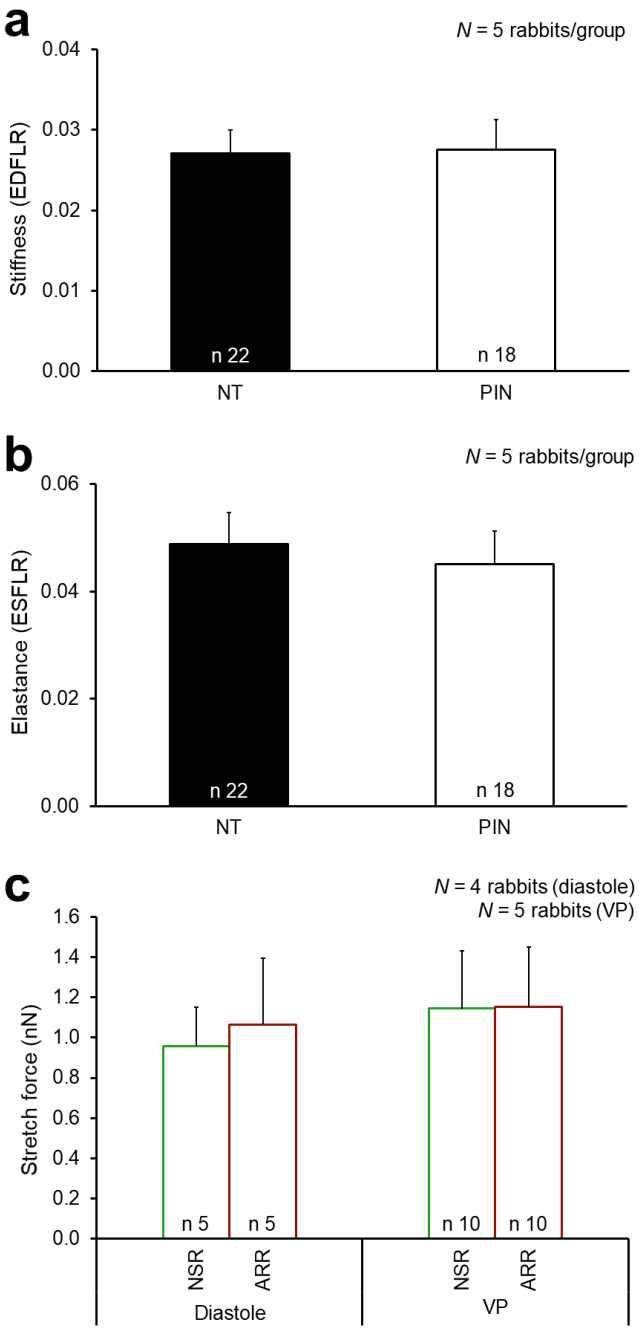

SUPPLEMENTARY INFORMATION

Supplementary Video 1 | Stretch-induced premature ventricular contraction. Example of rapid, transient stretch of a rabbit isolated ventricular myocyte treated with pinacidil, applied using microscopic carbon fibres adhered to either end of the cell, which resulted in a premature ventricular contraction. Sarcomere dynamics and carbon fibre positions were simultaneously measured to assess arrhythmic incidence and confirm maintenance of contractile function (representative sarcomere trace shown in Fig. 2b).

Supplementary Video 2 | Stretch-induced premature ventricular asystole. Example of rapid, transient stretch of a rabbit isolated ventricular myocyte treated with pinacidil, applied using microscopic carbon fibres adhered to either end of the cell, which resulted in asystole. Sarcomere dynamics and carbon fibre positions were simultaneously measured to assess arrhythmic incidence and confirm maintenance of contractile function (representative sarcomere trace shown in Fig. 2d).

Supplementary Video 3 | Stretch-induced sustained arrythmia with termination by stretch. Example of rapid, transient stretch of a rabbit isolated ventricular myocyte treated with pinacidil, applied using microscopic carbon fibres adhered to either end of the cell, which resulted in a sustained arrhythmia that was terminated by application of a second stretch. Sarcomere dynamics and carbon fibre positions were simultaneously measured to assess arrhythmic incidence and confirm maintenance of contractile function (representative sarcomere trace shown in Fig. 2f).

Supplementary Video 4 | Stretch-induced, calcium-driven sustained arrhythmia. Example of simultaneous voltage (blue)-calcium (red) fluorescence imaging in a rabbit isolated ventricular myocyte treated with pinacidil. Rapid, transient stretch during the vulnerable period (green bar) resulted in sustained arrhythmic activity, in which oscillations in intracellular calcium preceded changes in voltage, indicating calcium-driven activity (see inset).